Title: Quantifying Rhythmic and Arrhythmic Components of Brain Activity

Authors: Jason da Silva Castanheira[1*], Mathieu Landry[2], Stephen M. Fleming[1,3,4]

Affiliations:
[1] Department of Experimental Psychology and Institute for Cognitive Neuroscience, University College London, 17-19 Alexandra House, London WC1N 3AZ, UK
[2] École de Psychologie, Université Laval, Québec, QC G1V 0A6, Canada
[3] Max Planck UCL Centre for Computational Psychiatry and Ageing Research, University College London, London WC1B 5EH, UK
[4] Canadian Institute for Advanced Research (CIFAR), Brain, Mind and Consciousness Program, Toronto, ON M5G 1M1, Canada

[*] Corresponding author: j.castanheira@ucl.ac.uk

Abstract:

Brain activity comprises both rhythmic (periodic) and arrhythmic (aperiodic) components. These signal elements vary across healthy aging, and disease, and may make distinct contributions to conscious perception. Despite pioneering techniques to parameterize rhythmic and arrhythmic neural components based on power spectra, the methodology for quantifying rhythmic activity remains in its infancy. Variation in analytical choices for isolating brain rhythms from background arrhythmic activity makes interpreting findings across studies difficult. Whether current approaches can accurately recover the independent contribution of these neural signal elements remains to be established. Here, using simulation and parameter recovery approaches, we show that standard analytic methods for quantifying rhythmic activity conflate these two neurophysiological components, yielding spurious correlations between spectral model parameters. We propose an alternative approach to overcome these limitations and demonstrate effective separation of rhythmic and arrhythmic components in simulated neural time series. We validate these methods using resting-state recordings from a large cohort. Our recommendations for spectral parameterization enable the robust independent quantification of rhythmic and arrhythmic signal components for cognitive neuroscience.

Keywords
Neurophysiology, Spectral analysis, Parameterization of spectra, Rhythmic, Arrhythmic, Oscillations.

Introduction

Brain activity is composed of both rhythmic (periodic) and arrhythmic (aperiodic) signal components observed across spatiotemporal scales (Buzsáki & Draguhn, 2004; Buzsáki & Watson, 2012; Donoghue et al., 2020). Rhythmic signal components appear as peaks in the frequency domain that sit above the arrhythmic background (Buzsáki et al., 2013; Donoghue et al., 2020; Wen & Liu, 2016; L. E. Wilson et al., 2022, 2024). Quantifying rhythmic oscillations and relating these rhythms to behaviour has been a longstanding goal of neuroscientific research (Berger, 1929; Herrmann et al., 2016). Oscillations in cortical field potentials are amenable to computational modelling (Breakspear et al., 2010; H. R. Wilson & Cowan, 1972), are theorized to relate to the synchrony of populations of neurons (Baillet, 2017; Buzsáki et al., 2012; Wang, 2010), and are believed to organize brain activity temporally and spatially (Fries, 2005; Schölvinck et al., 2010; Singer, 2013; Varela et al., 2001). Over a century of research (Mushtaq et al., 2024) has shown that brain rhythms relate to perceptual and cognitive processes (Arnal & Giraud, 2012; Baillet, 2017; Samaha et al., 2020a), can differentiate individuals from one another (Castanheira et al., 2024; da Silva Castanheira et al., 2021; da Silva Castanheira, Poli, et al., 2024), and are altered by neurological and psychiatric diseases (Gallego-Rudolf et al., 2024; Heinrichs-Graham et al., 2014; Wiesman, Castanheira, et al., 2022; Wiesman et al., 2023).

Arrhythmic signal components, in contrast, are characterized by a power law ($1/f^{x}$) distribution in frequency space (Donoghue et al., 2020; Gao et al., 2017). The arrhythmic signal component has been traditionally treated as background noise, and something to be removed (Donoghue et al., 2020; Groppe et al., 2013). More recent investigations, however, challenge this viewpoint and suggest that the arrhythmic spectral component fluctuates alongside the demands of cognitive tasks (Cunningham et al., 2023; Gyurkovics et al., 2022; Waschke et al., 2021), reflects behavioural traits (Lu et al., 2024; B. D. Ostlund et al., 2021), accounts for the observation of flatter power spectra with

increasing age (Voytek et al., 2015; L. E. Wilson et al., 2022), and is altered by disease (da Silva Castanheira, Wiesman, et al., 2024; Donoghue, 2024; Wiesman et al., 2023). In addition, recent computational work and growing empirical evidence have led to the hypothesis that the arrhythmic exponent reflects a physiological balance between excitatory (E) and inhibitory (I) neural activity – a core property of brain dynamics that shapes neural computation, information flow, and network stability (Brake et al., 2024; Chini et al., 2022; Gao et al., 2017; Maschke et al., 2023; Weijs et al., 2025; Wiest et al., 2023).

Other work has explored how both arrhythmic and rhythmic neurophysiological activity correlates with behaviour. Take, for example, how pre-stimulus brain activity predicts participants' conscious perception of an upcoming stimulus. While previous research has emphasized the importance of peristimulus alpha brain rhythms (8-12 Hz) in predicting subjective experience and confidence judgments (Samaha et al., 2017; Wöstmann et al., 2019) in both visual and auditory domains, more recent evidence suggests that arrhythmic signal elements also relate to participants' awareness of upcoming stimuli. This has led to a recent hypothesis that these two neural signal components independently predict awareness judgments (Koenig & He, 2025).

Despite a growing interest in understanding the behavioural and mechanistic consequences of arrhythmic brain activity, the methodology for distinguishing rhythmic from arrhythmic activity remains in its infancy. Previous work relied on measures of relative power, which do not account for the power law ($1/f^{\chi}$) background activity, muddying the relationship between rhythmic and arrhythmic components (Davidson et al., 2022; Rempe et al., 2023; Samaha et al., 2022). Other researchers advocate for spectral detrending approaches which rely on computational modelling, such as *specparam*, which decomposes power spectra into their constituent signal elements (Donoghue et al., 2020; Wen & Liu, 2016; L. E. Wilson et al., 2022, 2024). The *specparam* model and its derivatives assume that neural power spectra are composed of independent contributions from rhythmic and arrhythmic activity, which are in turn associated with unique model parameters (i.e., the 1/f slope and Gaussian peaks)

(Donoghue et al., 2020; Medrano et al., 2025; L. E. Wilson et al., 2022, 2024). The *specparam* algorithm iteratively searches for Gaussian rhythmic peaks that sit above the power law ($1/f^{\chi}$), and parametrizes their centre frequency, amplitude, and bandwidth. The height of these Gaussian peaks (i.e., amplitude) reflects the total power of a given brain rhythm (Figure 1b). In addition, the arrhythmic signal component is characterised by two parameters: the offset and slope (i.e., exponent; χ). These signal elements are summed together in the frequency domain to generate the broadband signal observed in neurophysiological recordings (Donoghue et al., 2020; L. E. Wilson et al., 2024).

Even within model-based approaches, methodological choices differ: some papers use the Gaussian height parameters from the *specparam* model as a measure of rhythmic power (Donoghue et al., 2020; Hill et al., 2022; B. Ostlund et al., 2022; Wiest et al., 2023), whereas others quantify the residual variance after subtracting the arrhythmic component from the neural power spectrum, either in log-log or linear space (i.e., detrending analyses) (da Silva Castanheira, Wiesman, et al., 2024; Lu et al., 2024; Merkin et al., 2022, 2023; Wiesman et al., 2023). Recent findings even question data-driven detrending approaches altogether (Brake et al., 2024). Brake et al. suggest that changes in arrhythmic activity impact spectral peaks in both a multiplicative and additive manner, requiring two distinct forms of detrending depending on the assumed physiological mechanism (i.e., detrending in log or linear space). Accordingly, and in contrast to the recommendations of the *specparam* algorithm, Brake et al. suggest that spectral detrending should be avoided when clear oscillatory peaks are present (Brake et al., 2024). More generally, the impact of these methodological choices on the decomposition of rhythmic and arrhythmic activity, and how they affect the conclusions drawn about links to behaviour, remains unknown. Without clear, evidence-based guidelines on how to appropriately decompose brain rhythms, the robustness, reproducibility, and interpretability of findings in the field remain underspecified.

Here we sought to explore how methodological choices in quantifying rhythmic activity from neural power spectra impact the interpretability of findings – first in simulation, and then in resting-state MEG recordings. Relying on simulated neural time series, we tested

whether the estimated correlation between spectral model parameters recovered the ground truth for various approaches to distinguishing rhythmic and arrhythmic components. Our goal was to verify the robustness of various methods for quantifying rhythmic brain activity and demonstrate how analytical choices can yield diverging interpretations of empirical data.

Methods

Measures of rhythmic power: Rhythmic brain activity within a narrow frequency band (e.g. alpha 8-12 Hz) was estimated as either i) modelled power, or detrended power in ii) log-log space and iii) linear space (see Figure 1b). Modelled power consisted of the height of the Gaussian peak fit by the *specparam* algorithm within a pre-defined frequency range. In the case of multiple fitted Gaussian peaks, we retained the Gaussian peak of the highest amplitude. If *specparam* fit no Gaussian peak within the frequency band of interest, we assigned the amplitude a value of NaN or 0 (see Simulations of neural time series for further exploration of how to deal with missing values). For detrended spectral power, we relied on previous definitions of rhythmic activity as the residual variance in the observed power spectrum after subtracting the modelled 1/f arrhythmic component. Note that the subtraction between the observed spectrum and arrhythmic power can be in either linear or log-log space. We defined rhythmic power as the mean power of this residual variance within a pre-defined frequency range (e.g., 8-12 Hz for the alpha band; Figure 1b, bottom panel).

Simulations of neural time series: We generated 16,000 simulated neural time series with a range of arrhythmic and rhythmic parameters. Neural time series were synthesized using the NeuroDSP toolbox, lasted 30 seconds, and had a sampling rate of 500 Hz. The choice of a brief 30-second recording was informed by previous empirical research, which establishes that brief 30-second recordings yield stable estimates of the power spectrum (da Silva Castanheira et al., 2021; Wiesman, da Silva Castanheira, et al., 2022). The range of rhythmic and arrhythmic parameters used to generate the synthetic data was

based on those extracted from the CamCAN dataset and previous computational work (see Empirical dataset for details) (L. E. Wilson et al., 2024).

Figure 1a depicts a schematic of the analysis pipelines applied to the simulated neural time series. First, to explore whether methodological choices in quantifying rhythmic activity lead to spurious relationships between the different parameters of the *specparam* model, we ran three sets of simulations. We manipulated either i) arhythmic exponent, ii) alpha amplitude, or iii) alpha centre frequency while holding all other parameter values constant. Within the simulated time series, there was no systematic relationship between arrhythmic exponent and rhythmic alpha power. Any significant correlation between these estimated components would therefore reflect a systematic bias introduced by the method chosen to quantify rhythmic activity.

We simulated 500 unique time series for each alpha amplitude, which ranged from 0.3 to 2.0 in steps of 0.2, with the alpha centre frequency and bandwidth held constant at 10 Hz and 2 Hz, respectively. We set the arrhythmic exponent to 1.0. Next, we simulated 500 unique time series for alpha centre frequencies ranging from 7 to 14 Hz in steps of 1 Hz. Alpha amplitude and arrhythmic exponent were held constant at 0.7 and 1.0, respectively. Finally, we simulated 500 unique time series for each value of the arrhythmic exponent, which varied from 0.6 to 1.5 Hz^{-1} in steps of 0.1 Hz^{-1}. Alpha centre frequency, amplitude, and bandwidth were held constant for these simulations. For all of these simulations, we included a constant beta peak of 19 Hz, with an amplitude of 0.4 a.u. and a bandwidth of 5 Hz.

Second, we tested whether the method for quantifying rhythmic brain activity impacts the recovery of a monotonic relationship between arrhythmic exponent and rhythmic alpha activity. To do so, we simulated 100 neural time series for 10 different effect sizes representing the relationship between alpha amplitude and arrhythmic exponent, starting from ρ= 0.0 up to ρ= 0.9 in steps of 0.1. Alpha amplitude ranged from 0.1 to 1.1 a.u., and arrhythmic exponent ranged from 0.5 to 1.5 Hz^{-1}. Beta centre frequency, amplitude, and bandwidth were held constant at 19 Hz, 0.4 a.u. and 5Hz, while alpha centre frequency

and bandwidth were held constant at 10 Hz and 2 Hz, respectively. We tested whether the recovered correlation between spectral parameters matched the simulated ground truth for the three methodologies of computing rhythmic alpha power—i.e., modelled power, log- and linear- detrending.

In a complementary analysis, we assessed the impact of missing values on the recovered relationships between alpha power and arrhythmic slope by either excluding data or replacing missing data with zero amplitude peaks. When defining rhythmic power as the height of the modelled Gaussian peak of *specparam*, users must decide whether to ignore spectra that do not contain a modelled peak within a pre-defined narrow band range of interest (e.g., the alpha band) or whether to replace missing values with zero (i.e., reflecting a Gaussian peak of height 0 above the arrhythmic background activity). The results of these analyses are presented in Figure 4.

Finally, we tested how the choices made in quantifying rhythmic brain activity impact the relationship between rhythmic alpha power and demographic variables (e.g. age) by synthesizing 100 neural time series for 10 different effect sizes. The relationship between alpha amplitude and the simulated demographic variable ranged from $\rho = 0.0$ up to $\rho = 0.9$ in steps of 0.1, with a fixed arrhythmic exponent of 1.0. We held the alpha centre frequency and bandwidth constant at 10 Hz and 2 Hz, respectively. Beta centre frequency, amplitude, and bandwidth were fixed at 19 Hz, 0.4 a.u., and 5Hz. We tested the effect of the three methodologies of computing rhythmic alpha power, as well as the impact of missing values on the recovered relationships. Results are presented in Figure S4.

<u>Parameterization of neural power spectra:</u> To quantify the contribution of arrhythmic and rhythmic components to both empirical and synthetic time series, we parameterized power spectra using the *ms-specparam* tool in Brainstorm (Donoghue et al., 2020; Tadel et al., 2011; L. E. Wilson et al., 2024). We parameterized power spectra between 1 and 50 Hz for the simulated data and between 1 and 40 Hz for the empirical MEG data. Hyperparameters for spectral modelling were as follows: a minimum peak height of 0.1

a.u., a maximum of 6 peaks, peak width limits between [1, 12] Hz, and a Gaussian overlap threshold of 0.75 s.d. for the empirical dataset and 2.0 for the simulated data. The choice of hyperparameter settings was informed by visual inspection of the data. The most parsimonious spectral model was selected according to the Bayesian Information Criterion.

Empirical dataset: Data of 606 participants from the Cambridge Centre for Aging and Neuroscience repository (CamCAN) were used to validate our results obtained in simulation (mean age = 54.69, SD = 18.28; 299 female) (Taylor et al., 2017). Each participant completed a resting-state, eye-closed MEG recording using a 306-channel VectorView MEG system (MEGIN, Helsinki, Finland) that lasted approximately 8 minutes. MEG data were collected using 102 magnetometers and 204 planar gradiometers sampled at 1 kHz with a 0.03-330 Hz bandpass filter.

MEG preprocessing: We preprocessed the magnetoencephalography (MEG) recordings using Brainstorm (March 2021 distribution) (Tadel et al., 2011) in MATLAB (2020b; Natick, MA), adhering to established best-practice guidelines (Gross et al., 2013). The preprocessing methodology followed the protocols detailed previously in (Castanheira et al., 2024; da Silva Castanheira et al., 2021; L. E. Wilson et al., 2024).

Data were filtered to remove i) line noise artifacts at 50 Hz and its first 10 harmonics, ii) an 88-Hz artifact present in the Cam-CAN dataset (Wiesman, da Silva Castanheira, et al., 2022), and iii) slow-wave and DC-offset artifacts using a high-pass finite impulse response (FIR) filter with a cutoff frequency of 0.3 Hz. To mitigate the impact of cardiac artifacts, low-frequency (1–7 Hz) and high-frequency (40–400 Hz) artifacts, we applied Signal-Space Projections (SSPs) and removed the first projector, which explained the most variance.

Neural time series were co-registered to the individual T1-weighted MRI of each participant, facilitated using approximately 100 digitized head points. Biophysical head models were computed using *Brainstorm*'s overlapping-spheres model (default parameters), and source models were computed using linearly constrained minimum-

variance (LCMV) beamforming following *Brainstorm*'s default parameters (2018 version for source estimation processes). Orientations of the 15,000 sources were constrained normal to the cortical surface. Neural power spectra were then computed using the Welch's method, utilizing 2-second windows with a 50% overlap for every region of the Destrieux atlas (Destrieux et al., 2010).

Statistics: We calculated Spearman correlations and 95% confidence intervals using the DescTools package in R (R Core Team, 2022). We computed the Spearman correlation between rhythmic power and arrhythmic exponent in Figure 2, between rhythmic alpha and beta power in Figure 3, between rhythmic alpha power and exponent in Figure 4, and between simulated demographics and alpha power in Figure S4.

We computed the error in arrhythmic parameter estimates by subtracting the ground truth parameters used in simulating the neural time series from their estimated values. We then assessed the relationship between the error in arrhythmic parameters and estimated alpha power using regression models implemented in R. The results of these analyses are presented in Figure 3.

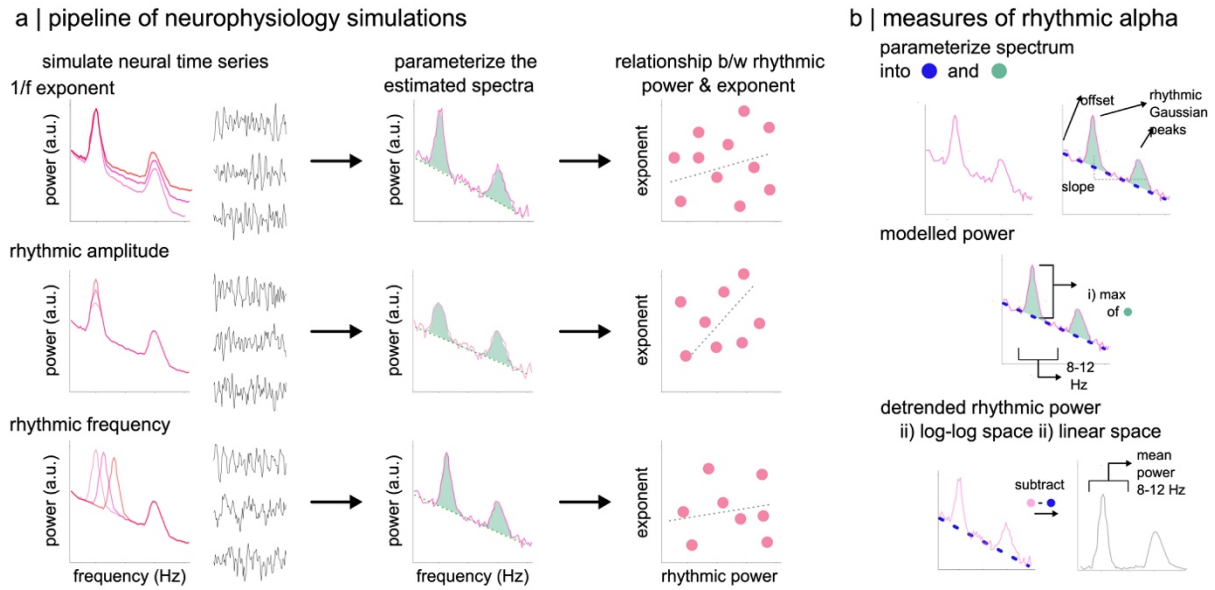

Figure 1: Schematic of simulations & definition of rhythmic power.
(a) Schematic of the pipeline of neural time series simulations. Neural time series data were simulated based on parameters of the *specparam* model in frequency space. These parameters included the slope of the 1/f arrhythmic activity (top panel), the amplitude of

rhythmic activity (middle panel) or the center frequency of rhythmic activity (bottom panel). We simulated neural time series with various ground truth relationships between the arrhythmic and rhythmic components. These simulated neural time series were transformed into the frequency domain and parameterized. The relationship between the simulated components was then evaluated based on the parameterized outputs.
(b) Schematic of different methodological choices for estimating rhythmic neural power. The rhythmic component of brain activity can be defined in three ways: i) as the maximum amplitude of modelled Gaussians within a defined frequency range (e.g., the alpha range 8-12 Hz), or detrended rhythmic power in ii) log-log space or iii) linear space.

Results

We simulated 16,000 neural time series across five experiments with known ground truth relationships between different spectral parameters of interest. We then asked how well three different methods for quantifying rhythmic brain activity could recover these simulated relationships. These three methods were denoted i) modelled power, ii) linear-detrended power and iii) log-detrended power (see Methods for details).

Spectral detrending introduces spurious correlations between arrhythmic and rhythmic components

In our first set of simulations, we evaluated the accuracy of each method in independently recovering the arrhythmic exponent and rhythmic alpha power. In these simulations, there was no ground truth correlation between these components (i.e., $\rho = 0$). As *specparam* characterises the contribution of Gaussian peaks independently of the 1/f background noise, we expected that modelled power would best recover this null relationship between the two signal components. In contrast, as detrending approaches depend on first modelling the neural power spectrum to accurately remove the contribution of the 1/f background noise, we hypothesized that this may introduce spurious correlations between the two signal components due to errors in model fit. We ran three sets of simulations varying i) alpha centre frequency, ii) alpha amplitude, and iii) arrhythmic exponent.

For the alpha centre frequency simulations, we observed that the choice of method to quantify rhythmic activity substantially impacted the recovered relationship between rhythmic alpha power and arrhythmic exponent. For modelled power, the observed

relationship between alpha power and exponent was generally close to the ground truth correlation of 0. Spearman correlation values were less than |0.15| for every simulated centre frequency except for 7 and 8 Hz, where we observed weak spurious relationships between alpha power and exponents (ρ = -0.18, CI [-0.27, -0.09]; -0.15 (CI [-0.24, -0.06], respectively) (Figure 2a left panel). Note that this difference in estimated correlation was not driven by a worse model fit (Figure S1). In comparison, we observed systematic spurious negative correlations between rhythmic and arrhythmic components (Spearman correlation values below -0.15) for both log- and linear-detrended methods. Log-detrended power performed the poorest of the three methods, with an average negative correlation between rhythmic alpha power and arrhythmic exponent of ρ =-0.35 (Figure 2a, middle panel). In contrast, the average estimated relationship between rhythmic alpha power and the arrhythmic exponent was ρ = -0.17 for linear-detrended power and ρ = -0.03 for modelled power (Figure 2a, left and right panels).

Next, we evaluated how well the three methods were able to recover a ground truth null relationship of alpha power and arrhythmic exponent for various simulated values of arrhythmic exponents, holding alpha centre frequency and amplitude constant (see Methods for details). Of the three methodologies for quantifying rhythmic alpha power, modelled power was the closest to ground truth with an average correlation between rhythmic alpha power and arrhythmic of ρ = 0.03, in comparison to ρ =-0.12 for linear-detrended power and ρ =-0.39 for log-detrended power (Figure 2b). The value of the simulated arrhythmic exponent did not substantially impact the estimated relationship between exponent and alpha power for log-detrended power. A similar pattern of parameter recovery was obtained when varying alpha amplitude, reported in Supplemental Materials (see Figure S2). Taken together, these analyses suggest that modelled power is the most robust method for quantifying rhythmic alpha power independently of arrhythmic brain activity.

Given the spurious relationships obtained between rhythmic alpha power and arrhythmic exponent, we next explored whether methodological choices in quantifying rhythmic brain activity may introduce similarly spurious relationships between different

brain rhythms. To this end, we explored recovery of linear monotonic relationships between estimates of rhythmic alpha (8-12 Hz) and beta power (12-24 Hz) for the three methods of computing rhythmic power. Akin to the previous results, we observed spurious positive correlations between alpha and beta amplitudes for log-detrended power (*log-log* mean $\rho = 0.54$) and linear-detrended power (*linear* mean $\rho = 0.44$; see Figure 2c). In contrast, for modelled power, alpha and beta power were generally unrelated to one another across simulations of various arrhythmic exponents (mean $\rho = 0.11$) and therefore closer to the ground truth of zero correlation. The spurious relationship between rhythmic alpha and beta power increased in strength for linear-detrended power (Figure 2c, right panel); we attribute this to the increasing influence of background signals on neural activity with larger arrhythmic exponents.

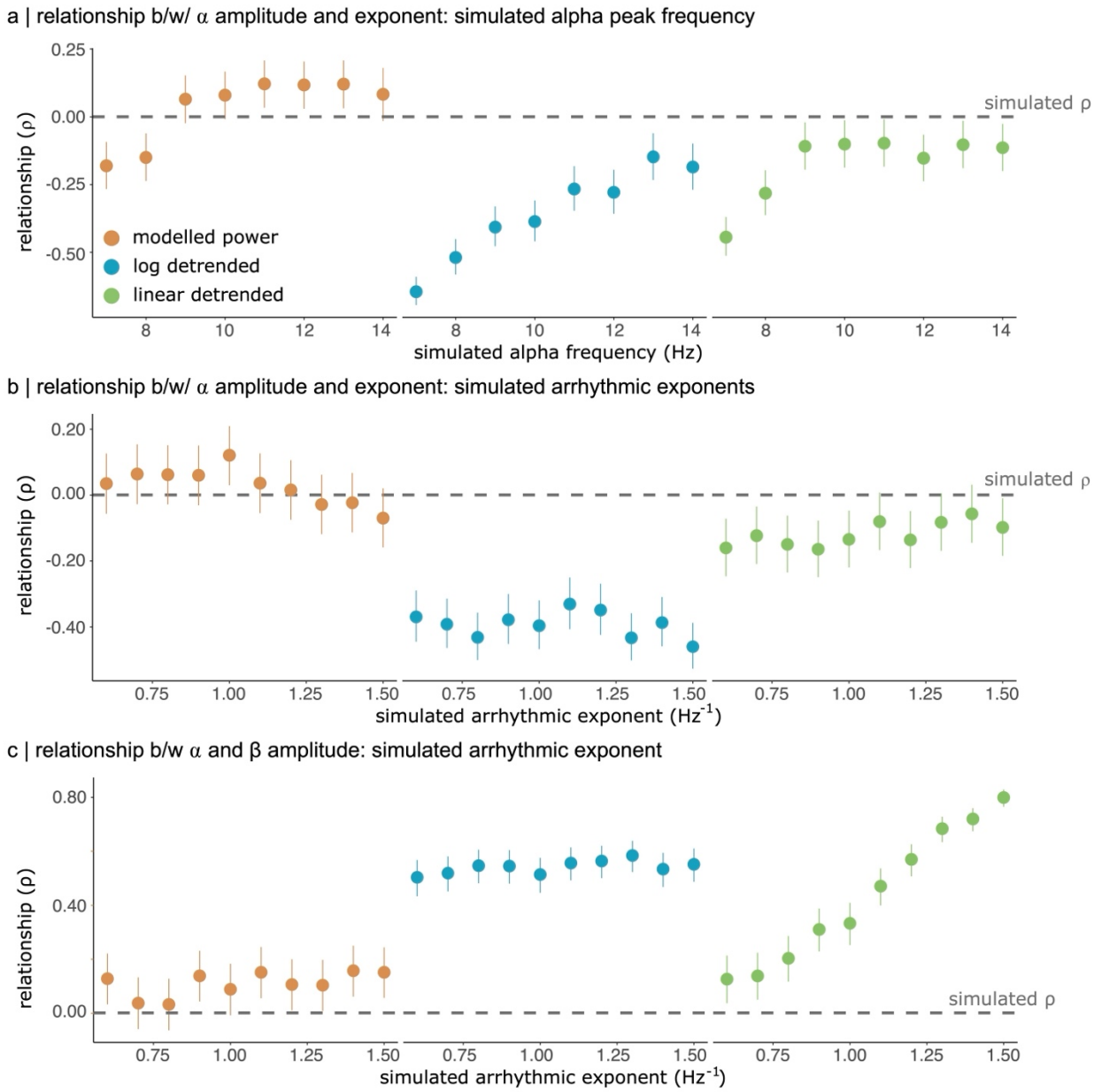

Figure 2: Spectral detrending induces spurious correlations between spectral model outputs.

(a) Estimated correlation between rhythmic alpha power and arrhythmic exponent at various simulated alpha center frequencies. The ground truth correlation is zero, indicated by the dotted line. Modelled power computed as the maximum amplitude of modelled Gaussian peaks is closer to the ground truth relationship between simulated alpha power and exponent (i.e., ρ =0.00). Spurious negative correlations of large magnitude ($\rho < -0.40$) between alpha power and arrhythmic exponent were obtained for log-detrended power. This is especially evident when the center frequency of the alpha oscillation lies at the edge of the narrow-band definition (i.e., 7-8 Hz).

(b) Estimated correlation between rhythmic alpha power and arrhythmic exponent for various levels of simulated arrhythmic exponents. Modelled alpha power recovers the ground truth relationship significantly better than detrending approaches. Log-detrended power induced large spurious correlations between alpha power and arrhythmic exponent for all simulated values of the arrhythmic exponent.
(c) Scatter plot of the relationship between rhythmic alpha and beta power for various simulated arrhythmic exponents. While synthetic time series data were simulated to have no linear relationship between alpha and beta amplitudes, spurious correlations were obtained between alpha and beta band power for log- and linear-detrending methods. In contrast, modelled power (left-most panel) shows no such spurious relationship between alpha and beta power, accurately recovering the ground truth null correlation between these parameters. Error bars represent 95% CI.

Error in spectral parameter estimates introduces spurious correlations between signal components

Next, we explored why detrending approaches—particularly in log space—result in spurious correlations between spectral parameter outputs. We hypothesized that errors in the estimated arrhythmic model parameters could explain the observed relationships between rhythmic and arrhythmic model parameters. To test this hypothesis, we fit a linear regression model where we predicted estimates of detrended power from the error in the arrhythmic parameter estimate (see Methods for details).

We observed that for spectra in which the arrhythmic offset was underestimated, log-detrended alpha power was also estimated as larger (β =0.30, SE =1.36 * 10^{-2}, $p < 0.001$, CI [0.27, 0.32]), with the largest errors in estimates of offset yielding alpha power estimates closest to the ground truth (dashed line Figure 3a top panel). We attribute this effect to the underestimation of alpha power using log-detrending approaches (i.e., most points fall below the dashed horizontal line in Figure 3a). In contrast, error in estimates of the arrhythmic slope showed a nonlinear quadratic relationship to log-detrended alpha power, for which the larger the absolute error in arrhythmic exponent, the higher the alpha power estimate (β =0.63, SE =1.09 * 10^{-2}, $p < 0.001$, CI [0.61, 0.65]). Error in both arrhythmic parameters independently predicted alpha power estimates (offset: β = 0.08, SE =1.25 * 10^{-2}, $p < 0.001$, CI [0.06, 0.11]; exponent: β = 0.61, SE =1.15 * 10^{-2}, $p < 0.001$, CI [0.59, 0.63]).

In contrast, we observed weak significant relationships between modelled alpha power and error in arrhythmic parameter estimates (offset: $\beta = -0.08$, SE $=1.68 * 10^{-2}$, $p < 0.001$, CI [-0.13, -0.06]; exponent: $\beta = 0.15$, SE $=1.55 * 10^{-2}$, $p < 0.001$, CI [0.12, 0.18]; see Figure 3a bottom panel). Note that although these relationships were statistically significant, they explained only a modest amount of total variance in modelled alpha power (3% of the variance in comparison to 42% of the variance in detrended alpha power), explaining why this method was largely successful in independently recovering these components.

Two example power spectra can be used to illustrate this effect. In the top panel of Figure 3b, a simulated neural power spectrum has been correctly modelled with two rhythmic peaks in the alpha and beta range, as well as an appropriate arrhythmic model. As a result, the detrended spectrum, plotted as the inlaid line graph, is unbiased. In contrast, when arrhythmic parameter estimates are incorrectly estimated as depicted in the bottom panel of Figure 3b, the detrended rhythmic power is greater than expected (Figure 3b bottom panel inlaid graph) – in this example, rhythmic power in lower frequencies is overestimated because of the underestimation of the arrhythmic offset. Detrending analyses are significantly more sensitive to errors in the arrhythmic model and, as a result, may introduce spurious relationships between estimated rhythmic and arrhythmic components.

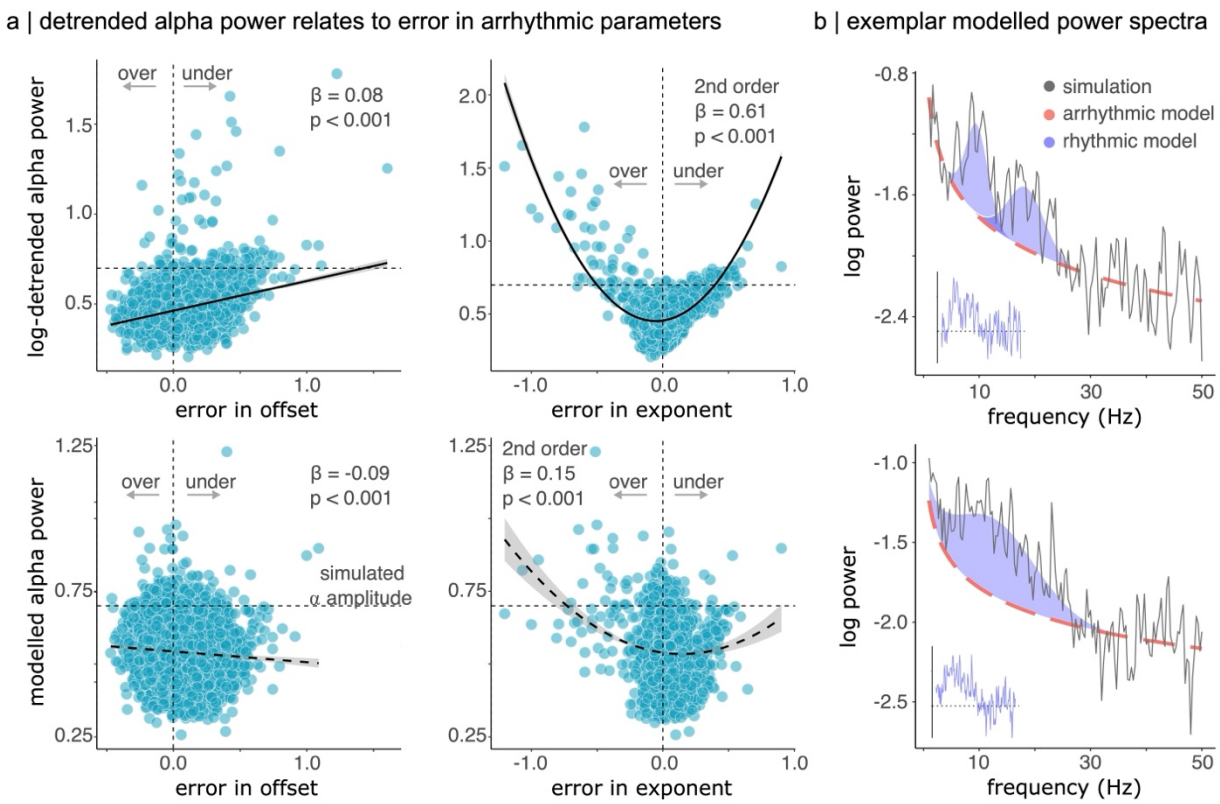

Figure 3: Error in arrhythmic parameter estimates predicts corrected but not modelled alpha power.

(a) Scatter plot of the relationship between alpha power (top panel, log-detrended power; bottom panel, modelled power) and error in the estimate of arrhythmic parameters. Log-detrended alpha power is linearly related to error in the arrhythmic offset, with larger estimates of alpha power observed for underestimated values in arrhythmic offset. Error in arrhythmic exponent nonlinearly related to alpha power, with extreme under- and over-estimated values of the exponent predicting large alpha power. Dashed lines indicated the simulated (ground truth) alpha power, and zero error along the y- and x- axis respectively. Modelled alpha power does not meaningfully relate to error in arrhythmic parameters.

(b) Example neural power spectra. The top panel depicts an accurately modelled power spectrum, while the bottom panel illustrates a poorly parameterized power spectrum. Black lines indicate the simulated spectrum, the red dashed line the arrhythmic model, and the inlaid blue line the detrended alpha power. Modelled rhythmic Gaussians sit atop the modelled arrhythmic slope—together they compose the *specparam* model.

Handling instances where *specparam* fails to model a peak

A specific disadvantage of modelled power, relative to detrending methods, is that it introduces missing values when the *specparam* algorithm fails to fit a Gaussian peak within a pre-defined narrow band frequency range (e.g., the alpha band). We therefore sought to explore the influence of these missing values on the recovered relationship between arrhythmic exponent and alpha power. We simulated 100 neural time series for 10 effect sizes describing the relationship between alpha power and arrhythmic exponent (from $\rho = 0.00$ to $\rho = 0.90$ in steps of 0.10). We observed that modelled power, on average, recovered the ground truth simulated relationship between alpha power and arrhythmic exponent (Figure 4a). We note, however, that larger effect sizes ($\rho > 0.50$) were systematically underestimated. We then tested the influence of replacing missing peak amplitudes not modelled by *specparam* with a value of 0.00. On average, estimated relationships between alpha amplitude and arrhythmic exponent were closer to the ground truth when missing peak amplitudes were replaced with zeros (Figure 4b).

Log-detrended power was similarly capable of recapitulating the simulated relationship between alpha power and arrhythmic exponent (Figure 4c). In contrast, linear-detrended power systematically overestimated the relationship between arrhythmic exponent and alpha power, principally for weaker relationships (Figure 4d). We also simulated the relationship between alpha power and a synthetic demographic variable and observed qualitatively similar results (see Figure S4 details).

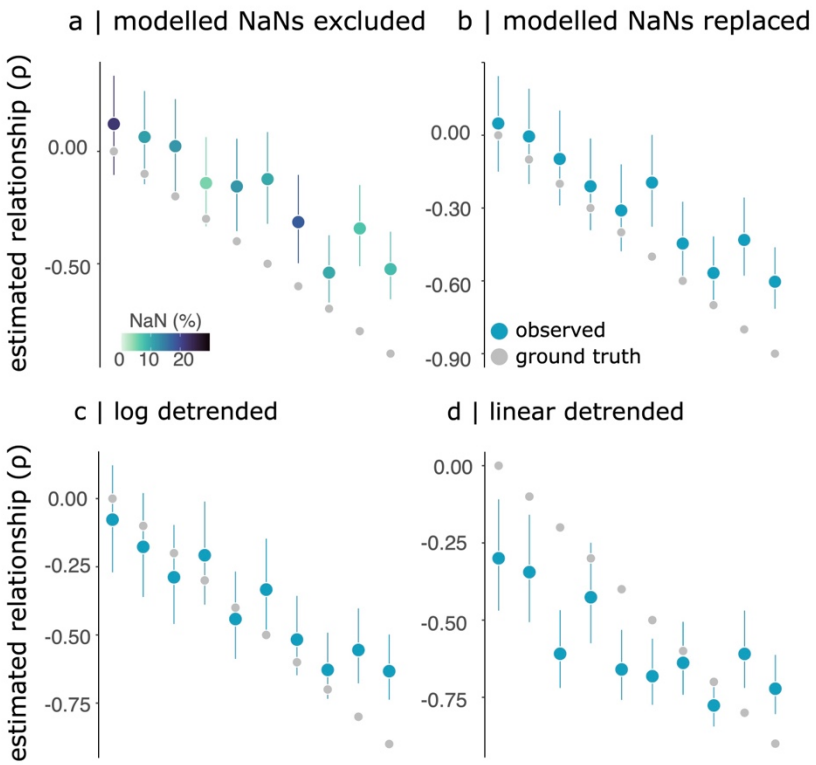

Figure 4: Replacing missing values with zeroes recovers simulated relationships.

Simulated relationships between rhythmic alpha power and arrhythmic exponent for various effect sizes across the three methods of extracting alpha power. Ground truth values (grey dots) represent the simulated relationship between the two parameters used to generate neural time series data. Blue dots represent the estimated relationship between rhythmic alpha power and arrhythmic exponent for modelled power. Modelled power recovers the simulated relationship between alpha power and arrhythmic exponent reasonably well, except at the largest effect sizes (a). Modelled alpha power generates missing data when no Gaussian peak is fit within the alpha range. The colour of the dots represents the percentage of missing data for each simulation. The estimated relationships are closer to the ground truth when missing values of spectral peak amplitudes are replaced with zeroes (b) in comparison to excluding these values (a). Log-detrended alpha power similarly recovers the simulated relationships well (c). However, linear-detrended power systematically overestimates the strength of the linear relationship (d). Error bars represent 95% CI.

Modelled vs detrended rhythmic power leads to diverging interpretations

Taken together, our simulation analyses corroborate our hypothesis: modelled power outperforms detrending methods and accurately quantifies the independent contributions of rhythmic and arrhythmic brain activity. We next sought to verify our results obtained in

simulation in an empirical dataset. In particular, our goal was to highlight how different methods of quantifying rhythmic amplitude may yield diverging interpretations. We analyzed the relationship between alpha amplitude and arrhythmic exponent, two proposed markers of cortical inhibition, in the resting-state MEG data of 606 individuals within the CamCAN database (18-89 years old).

We estimated the linear monotonic relationship between resting-state arrhythmic exponents and alpha power using Spearman correlations for each of 148 cortical parcels of the Destrieux atlas. We observed a rostro-caudal gradient, with frontal brain regions showing a positive linear relationship and posterior areas having a negative relationship between log-detrended alpha power and arrhythmic exponent (Figure 5a, left panel). In contrast, the relationship between modelled alpha power and arrhythmic exponent was positive across the entire cortex, except within nine occipital parcels (Figure 5a left panel). See Figure S5 for FDR thresholded brain maps of this relationship. We then computed the linear relationship between alpha power and arrhythmic exponent for every parcel across three age groups (young adults 18-45, adults 45-65, and older adults 65+ years old). Notably, we observed that the method used to quantify rhythmic alpha amplitude meaningfully impacted the results (Figure 5b). Using the log-detrended power approach, we found that the relationship between alpha power and the arrhythmic exponent varied depending on the age group assessed. Older adults showed more positive correlations between alpha power and arrhythmic exponent compared to younger adults – an effect which was most pronounced in fronto-central and temporal brain regions. However, this dependency of spectral relationship on age disappeared for modelled alpha power, suggesting it may be a spurious consequence of the detrending approach (Figure 5b, bottom row).

We also examined the impact of these methodological choices on other individual differences. First, we observed strong positive relationships between rhythmic alpha and beta amplitudes when using log-detrended power – relationships which were not obtained for modelled power (Figure S7). When evaluated in combination with our simulation results, these findings suggest that detrending approaches may introduce spurious

correlations between brain rhythms. Second, we computed the relationship between alpha amplitude and chronological age, and observed that it, again, depended on the method of quantifying power (see Figure S6). Third, we observed that the relationship between the arrhythmic exponent and frontal log-detrended beta power inverts when relying on modelled beta power (see Figure S8). Together, our findings in the CamCAN dataset illustrate that the choice of method for quantifying rhythmic activity can yield diverging and potentially spurious results when applied to empirical data.

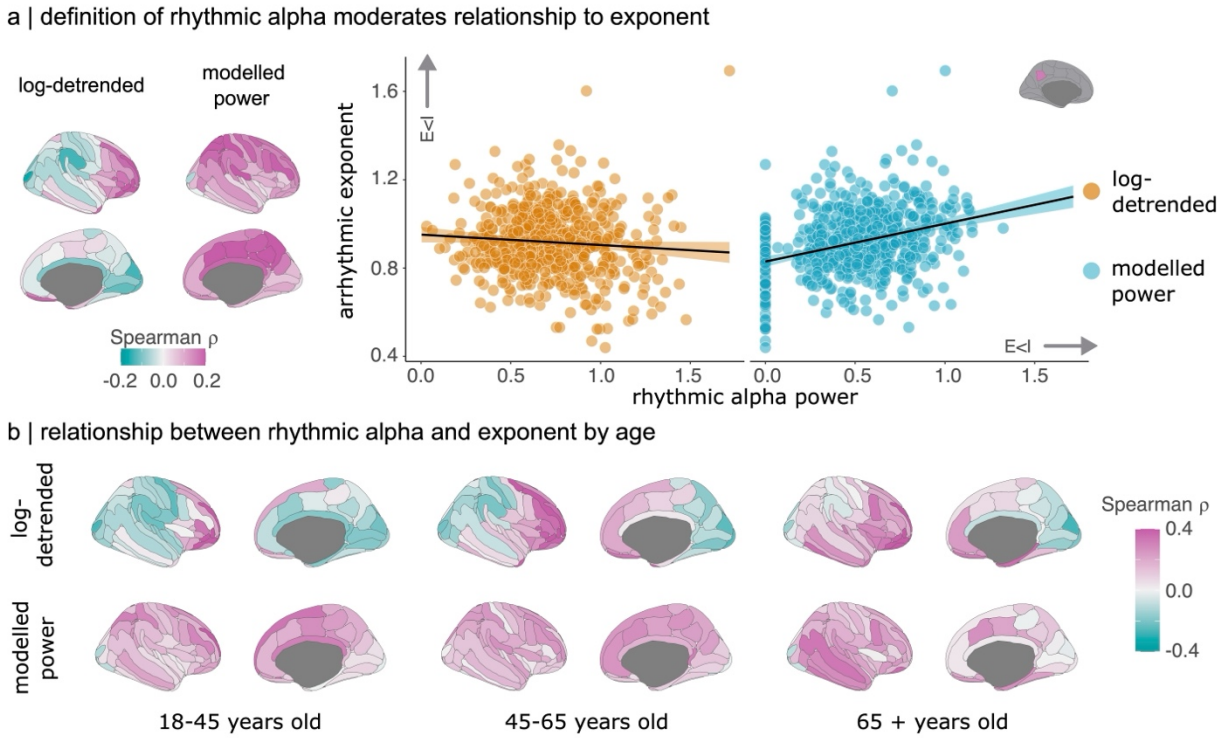

Figure 5: The choice of method for quantifying rhythmic power impacts obtained relationships between spectral components (empirical data).

(a) Left panel: Topographic map of the linear monotonic relationship between rhythmic alpha amplitude and arrhythmic exponent for log-detrended (left) and modelled alpha power. Log-detrended alpha power negatively relates to arrhythmic exponent, principally in posterior brain regions, including the visual cortex. In contrast, modelled alpha power positively relates to arrhythmic exponent across the entirety of the cortex, except for nine occipital regions. Right panel: Scatter plot of the relationship between rhythmic alpha power and arrhythmic exponent for an exemplar brain region. While log-detrended alpha power weakly negatively predicts arrhythmic exponent, modelled alpha power positively predicts arrhythmic exponent in this brain area. Note that the distribution of zero alpha

amplitude values reflects participants for whom *specparam* did not model a Gaussian peak.
(b) Topographic map of the linear monotonic relationship between rhythmic alpha amplitude and arrhythmic exponent for i) different age groups (columns) and ii) the two methods for quantifying rhythmic power (rows). The interpretation of the relationship between resting-state alpha power and arrhythmic exponent differs substantially depending on the method for quantifying the amplitude of alpha power.

Discussion

The analysis of brain rhythms is central to the field of neuroscience. For over a century, researchers have sought to establish links between neural oscillations, behaviour, and disease (Mushtaq et al., 2024). However, methods for quantifying rhythmic power vary considerably and make differing assumptions (Brake et al., 2024; Donoghue et al., 2020; Wen & Liu, 2016). We explored how the choice of method for computing the amplitude of brain rhythms impacts the recovery of simulated ground-truth relationships between different spectral features. Addressing this question is critical to establishing whether rhythmic and arrhythmic signal components differentially relate to behaviour. We demonstrate, based on simulated neural time series, that modelling Gaussian amplitudes (e.g. as implemented in *specparam*) provides a robust method for quantifying the power of brain rhythms independent of the arrhythmic exponent. Modelled power recovers independent sources of variance that are minimally contaminated by arrhythmic signal components. In contrast, linear and log detrending methods can introduce spurious relationships between arrhythmic and rhythmic parameters.

Is spectral detrending necessary?

Previous research has treated background 1/f brain activity as noise to be removed when quantifying the amplitude of brain rhythms. Spectral detrending or whitening is used to correct for this background activity, either by computing relative power or modelling the arrhythmic signal component (Donoghue et al., 2020). Despite the growing use of algorithms to parameterize the neural power spectra (Donoghue et al., 2020; Wen & Liu, 2016; L. E. Wilson et al., 2022, 2024), questions remain about whether researchers should detrend the power spectrum when clear oscillations are present. Indeed, recent computational modelling work suggests that spectra require different types of

detrending—i.e., dividing vs subtracting—depending on the specific physiological mechanisms one assumes to drive observed changes in the arrhythmic spectrum (Brake et al., 2024). Brake et al. (2024) concluded that spectral detrending should be avoided altogether unless a clear biophysical and physiological justification is provided. Yet the rhythmic components of the neural power spectra were not explicitly modelled using Gaussian peaks, as pursued in *specparam*. By ignoring dynamics in background brain activity, researchers may conflate arrhythmic signal components with narrow-band modulations of power. This latter point is of particular interest when testing for potential physiological correlates of behaviour.

The present paper explores this question with ground-truth simulations. Our findings suggest that modelling rhythmic activity by fitting Gaussian peaks recovers the simulated amplitude of neural oscillations with greater accuracy than detrending approaches, which are subject to biases (Figure 2). These biases are introduced when the arrhythmic component of the power spectrum is not accurately fit, leading to spurious correlations between model parameters (Figure 3). The spurious relationships observed in detrending analyses are not limited to rhythmic and arrhythmic exponents. We found that the amplitudes of different rhythmic oscillations are spuriously correlated if the background 1/f component of the spectrum is not adequately detrended (Figure 2c). This poses challenges for isolating the independent contribution of multiple brain rhythms.

The relationship between arrhythmic and rhythmic brain activity

Alpha power is theorized to reflect cortical inhibition, principally in the sensory cortex (Clayton et al., 2018; Foxe & Snyder, 2011; Jensen, 2024; Jensen & Mazaheri, 2010; Morrow et al., 2023; Samaha et al., 2020b). Phases of alpha power are believed to reflect periods of local inhibition and disinhibition, with increases in alpha amplitude believed to reflect increased cortical inhibition. Posterior alpha rhythms similarly predict the likelihood of reporting phosphenes triggered by transcranial magnetic stimulation (TMS), which is interpreted in support of the inhibition interpretation of alpha rhythms (Romei, Brodbeck, et al., 2008; Romei, Rihs, et al., 2008). Work on the orienting of attention corroborates

this theory, with decreased alpha power observed contralateral to the attended visual hemifield (Bagherzadeh et al., 2020; Jensen, 2024; Landry et al., 2024).

A separate line of work has proposed that the arrhythmic exponent reflects the relative contribution of excitatory and inhibitory populations of neurons. Several lines of evidence support this view: computational work suggests that the arrhythmic exponent reflects the relative contribution of AMPA and $GABA_A$ populations (Gao et al., 2017). Similarly, administration of anesthetics alters the slope of the arrhythmic component (Colombo et al., 2019; Lendner et al., 2020; Maschke et al., 2023; Waschke et al., 2021). Recent work leveraging a pupil-based biofeedback paradigm demonstrates that changes in the brain's state of arousal are correlated to shifts in cortical arrhythmic brain activity (Weijs et al., 2025).

These two threads in the literature suggest that the arrhythmic exponent and alpha power should be closely related, given the close link between cortical inhibition and the E-I balance. Yet, the relationship between alpha power and arrhythmic exponent remains largely unexplored. Our analysis of empirical data demonstrates how the interpretation of the relationship between alpha power and the arrhythmic exponent depends on the methodological choices. Log-detrending methods introduce a spurious negative relationship between arrhythmic exponents and alpha power signals at rest (see Figure 5a). In contrast, when using spectral modelling, we observed that alpha power and arrhythmic exponent are positively correlated (Figure 5b) across the adult lifespan, in line with what we would expect from theories of cortical inhibition. This observation dovetails with recent findings suggesting that the two signal components are positively correlated during a perceptual decision-making task (Elliott et al., 2025).

While our results speak to the shared variance between two hypothesized markers of inhibition, a substantial portion of variance remains to be explained. We speculate that different biophysical parameters may govern local inhibition (i.e., the conductance of channels versus the activity of inhibitory cell populations), which would explain why we did not observe that alpha power and the arrhythmic exponent are not more strongly

correlated with one another. In line with this interpretation, Brake and colleagues demonstrated using computational modelling that arrhythmic exponents may not be a reliable marker of E-I balance, given the nonlinearities of membrane dynamics (Brake et al., 2024). It is therefore likely that both signals reflect a cascade of complex neuronal functions, some of which reflect cortical inhibition. Future empirical and computational work should seek to clarify the biophysical underpinnings of both alpha rhythms and background 1/f activity.

Despite the theoretical interpretation of alpha power and the arrhythmic exponent as markers of cortical inhibition, *specparam* and related models assume that the contributions of arrhythmic and rhythmic signal components are independent (additive) of one another (Donoghue et al., 2020; Medrano et al., 2025; L. E. Wilson et al., 2022, 2024). Accordingly, our findings indicate that modelling Gaussian amplitudes can recover the independent contribution of arrhythmic and rhythmic signal components in simulation (Figure 2). However, future work may fruitfully explore whether a comprehensive neurophysiological generative model could explain the empirical relationships observed between alpha power and arrhythmic exponent at rest.

Rhythmic and arrhythmic correlates of conscious awareness and metacognition

The independent contribution of rhythmic and arrhythmic signal components to behaviour and disease is an ever-growing topic of research (Koenig & He, 2025; Wiesman et al., 2023). In the field of metacognition research, evidence suggests that both arrhythmic and rhythmic power, measured prior to stimulus onset, can predict participants' subjective visibility and confidence reports over and above variation in objective performance (Benwell et al., 2017; Cunningham et al., 2023; Limbach & Corballis, 2016; Samaha et al., 2017, 2020b, 2022; Wöstmann et al., 2019). Notably, the amplitude and phase of alpha rhythms before the presentation of a visual target predict participants' subsequent reports of visibility, but not their discrimination performance (Pilipenko & Samaha, 2024; Samaha et al., 2015, 2022). Others have proposed that individual differences in alpha centre frequencies (referred to as IAF in the field) predict the rhythm of conscious perception, governing the temporal window within which two stimuli are likely to be fused

into a single percept (Samaha & Postle, 2015; Samaha & Romei, 2024; Smit et al., 2006; Xu et al., 2025). Together, these results suggest that pre-stimulus alpha band activity in sensory cortex is critical for the timing and gating of subjective aspects of perception.

More recent investigations have explored the role of arrhythmic signals in conscious perception. It has been demonstrated that flatter pre-stimulus power spectra (i.e., smaller arrhythmic exponents) predict awareness of subsequent stimuli (Cunningham et al., 2023; Waschke et al., 2021). Moreover, work on subitizing capacity suggests that arrhythmic exponent, and not alpha peak frequency or power, predicted inter-individual differences in the number of items participants perceived (Elliott et al., 2025). This growing body of work corroborates the importance of considering arrhythmic signal components in the study of conscious perception. Whether the rhythmic and arrhythmic components of the pre-stimulus elements independently contribute to conscious awareness remains underdetermined. In a recent study, Koeing and He (2025) suggest that the rhythmic and arrhythmic components independently contribute to conscious awareness, with the influence of arrhythmic activity on conscious perception being partly explained by pupil-size related changes in arousal. In light of our present analyses, it will be important to test for the possibility of more complex relationships between arrhythmic signals and alpha power, and explore the hypothesis that both components reflect inhibitory processes which jointly contribute to conscious perception and metacognition.

Methodological Considerations

Based on our simulations, we recommend that researchers explicitly model Gaussian amplitudes when quantifying rhythmic power, using algorithms such as *specparam*. We show that this method minimizes the potential for spurious relationships between arrhythmic and rhythmic model parameters (Figure 2). One methodological consideration when using modelled power is the large number of missing data points that occur as a result of *specparam* failing to fit a spectral peak within a predefined narrow-band frequency range (e.g., alpha 8- 12 Hz). We investigated whether this disadvantage can be overcome by replacing the missing values with an amplitude of zero (e.g., Figure 4).

Our simulations suggest that this approach accurately recovers simulated relationships. We note, however, that this analytic choice may alter the distribution of the resulting data, rendering non-parametric statistics necessary. In addition, this approach of dealing with missing data only applies to the amplitude of rhythmic oscillations. In the case of center frequencies, for example, it remains unclear what the best approach is to deal with missing data.

Another methodological consideration is the use of pre-defined fixed ranges to delineate frequency bands of interest (e.g., alpha band 8- 12 Hz). There is considerable inter-individual diversity in brain rhythms, including the specific centre frequency of the rhythm. This makes aggregating data across individuals challenging, specifically if an individual's centre frequency falls at the edge of the canonical frequency band definitions. We observed in our simulations that centre frequencies at the lower edge of the pre-defined narrow-band may introduce spurious relationships between narrow-band estimates of rhythmic power and the arrhythmic exponent (see Figure 2a, modelled power). While these spurious relationships are much smaller in magnitude than the ones observed with detrending methods, we would advise researchers to explore inter-individual differences in the centre frequency of brain rhythms before defining a frequency band of interest.

In conclusion, we demonstrate that analytical choices when quantifying the amplitude of brain rhythms can lead to spurious correlations between arrhythmic and rhythmic spectral parameters and confound interpretations of findings. By relying on simulations of neural time series, we demonstrated that detrending approaches lead to misleading negative correlations between the arrhythmic exponent and alpha power. In contrast, modelled power provides the most robust approach for quantifying the amplitude of brain rhythms. Based on modelled Gaussian peaks, we show that arrhythmic exponents and alpha power are positively correlated across the cortex in individuals sampled from a large age range. In line with theories of cortical inhibition, our results suggest a possible unitary neural mechanism underlying both signal components. These findings, in turn, raise new questions about how these signal components contribute to conscious perception and metacognition. We anticipate that the findings of this paper will inform future research on

the neural mechanisms of these processes, encouraging more robust, reproducible, and interpretable results.

Data & code availability:

All in-house code used for data analysis and visualization is available on GitHub https://github.com/jasondsc/IndependenceArrhythmicRhythm. The reanalyzed data presented herein are available from https://cam-can.mrc-cbu.cam.ac.uk. The simulated neural time series are available upon reasonable request from the first author.

Declaration of Competing Interests:

All authors declare no competing conflicts of interest.

Author Contributions:

Conceptualization: J.d.S.C., M.L., and S.F.

Data Curation: J.d.S.C.

Methodology: J.d.S.C., M.L., and S.F.

Software: J.d.S.C.

Visualization: J.d.S.C., and S.F.

Validation: J.d.S.C.

Formal analysis: J.d.S.C.

Supervision: M.L., S.F.

Project administration: S.F.

Writing—original draft: J.d.S.C. and S.F.

Writing—review and editing: J.d.S.C., M.L., and S.B.

References:

Arnal, L. H., & Giraud, A.-L. (2012). Cortical oscillations and sensory predictions. *Trends in Cognitive Sciences*, *16*(7), 390–398. https://doi.org/10.1016/j.tics.2012.05.003

Bagherzadeh, Y., Baldauf, D., Pantazis, D., & Desimone, R. (2020). Alpha Synchrony and the Neurofeedback Control of Spatial Attention. *Neuron*, *105*(3), 577-587.e5. https://doi.org/10.1016/j.neuron.2019.11.001

Baillet, S. (2017). Magnetoencephalography for brain electrophysiology and imaging. *Nature Neuroscience*, *20*(3), Article 3. https://doi.org/10.1038/nn.4504

Benwell, C. S. Y., Tagliabue, C. F., Veniero, D., Cecere, R., Savazzi, S., & Thut, G. (2017). Prestimulus EEG Power Predicts Conscious Awareness But Not Objective Visual Performance. *Eneuro*, *4*(6), ENEURO.0182-17.2017. https://doi.org/10.1523/ENEURO.0182-17.2017

Berger, H. (1929). Über das elektroenkephalogramm des menschen. *Archiv Für Psychiatrie Und Nervenkrankheiten*, *87*(1), 527–570.

Brake, N., Duc, F., Rokos, A., Arseneau, F., Shahiri, S., Khadra, A., & Plourde, G. (2024). A neurophysiological basis for aperiodic EEG and the background spectral trend. *Nature Communications*, *15*(1), 1514. https://doi.org/10.1038/s41467-024-45922-8

Breakspear, M., Heitmann, S., & Daffertshofer, A. (2010). Generative Models of Cortical Oscillations: Neurobiological Implications of the Kuramoto Model. *Frontiers in Human Neuroscience*, *4*, 190. https://doi.org/10.3389/fnhum.2010.00190

Buzsáki, G., Anastassiou, C. A., & Koch, C. (2012). The origin of extracellular fields and currents—EEG, ECoG, LFP and spikes. *Nature Reviews Neuroscience*, *13*(6), 407–420. https://doi.org/10.1038/nrn3241

Buzsáki, G., & Draguhn, A. (2004). Neuronal Oscillations in Cortical Networks. *Science*, *304*(5679), 1926–1929. https://doi.org/10.1126/science.1099745

Buzsáki, G., Logothetis, N., & Singer, W. (2013). Scaling brain size, keeping timing: Evolutionary preservation of brain rhythms. *Neuron*, *80*(3), 751–764. https://doi.org/10.1016/j.neuron.2013.10.002

Buzsáki, G., & Watson, B. O. (2012). Brain rhythms and neural syntax: Implications for efficient coding of cognitive content and neuropsychiatric disease. *Dialogues in Clinical Neuroscience*, *14*(4), 345–367. https://doi.org/10.31887/DCNS.2012.14.4/gbuzsaki

Castanheira, J. da S., Wiesman, A. I., Taylor, M. J., & Baillet, S. (2024). *The Lifespan Evolution of Individualized Neurophysiological Traits* (p. 2024.11.27.624077). bioRxiv. https://doi.org/10.1101/2024.11.27.624077

Chini, M., Pfeffer, T., & Hanganu-Opatz, I. (2022). An increase of inhibition drives the developmental decorrelation of neural activity. *eLife*, *11*, e78811. https://doi.org/10.7554/eLife.78811

Clayton, M. S., Yeung, N., & Cohen Kadosh, R. (2018). The many characters of visual alpha oscillations. *The European Journal of Neuroscience*, *48*(7), 2498–2508. https://doi.org/10.1111/ejn.13747

Colombo, M. A., Napolitani, M., Boly, M., Gosseries, O., Casarotto, S., Rosanova, M., Brichant, J.-F., Boveroux, P., Rex, S., Laureys, S., Massimini, M., Chieregato, A., & Sarasso, S. (2019). The spectral exponent of the resting EEG indexes the presence of consciousness during unresponsiveness induced by propofol, xenon, and ketamine. *NeuroImage*, *189*, 631–644. https://doi.org/10.1016/j.neuroimage.2019.01.024

Cunningham, E., Zimnicki, C., & Beck, D. M. (2023). The Influence of Prestimulus 1/f-Like versus Alpha-Band Activity on Subjective Awareness of Auditory and Visual Stimuli.

Journal of Neuroscience, *43*(37), 6447–6459. https://doi.org/10.1523/JNEUROSCI.0238-23.2023

da Silva Castanheira, J., Orozco Perez, H. D., Misic, B., & Baillet, S. (2021). Brief segments of neurophysiological activity enable individual differentiation. *Nature Communications*, *12*(1), Article 1. https://doi.org/10.1038/s41467-021-25895-8

da Silva Castanheira, J., Poli, J., Hansen, J. Y., Misic, B., & Baillet, S. (2024). Genetic Foundations of Neurophysiological and Behavioural Variability Across the Lifespan. *bioRxiv*, 2024–07. https://doi.org/10.1126/sciadv.ads7544

da Silva Castanheira, J., Wiesman, A. I., Hansen, J. Y., Misic, B., Baillet, S., Breitner, J., Poirier, J., Bellec, P., Bohbot, V., & Chakravarty, M. (2024). The neurophysiological brain-fingerprint of Parkinson's disease. *EBioMedicine*, *105*. https://www.thelancet.com/journals/ebiom/article/PIIS2352-3964(24)00236-6/fulltext

Davidson, M. J., Macdonald, J. S. P., & Yeung, N. (2022). Alpha oscillations and stimulus-evoked activity dissociate metacognitive reports of attention, visibility, and confidence in a rapid visual detection task. *Journal of Vision*, *22*(10), 20. https://doi.org/10.1167/jov.22.10.20

Destrieux, C., FISCHL, B., DALE, A., & HALGREN, E. (2010). Automatic parcellation of human cortical gyri and sulci using standard anatomical nomenclature. *NeuroImage*, *53*(1), 1–15. https://doi.org/10.1016/j.neuroimage.2010.06.010

Donoghue, T. (2024). *A systematic review of aperiodic neural activity in clinical investigations* (p. 2024.10.14.24314925). medRxiv. https://doi.org/10.1101/2024.10.14.24314925

Donoghue, T., Haller, M., Peterson, E. J., Varma, P., Sebastian, P., Gao, R., Noto, T., Lara, A. H., Wallis, J. D., Knight, R. T., Shestyuk, A., & Voytek, B. (2020). Parameterizing neural

power spectra into periodic and aperiodic components. *Nature Neuroscience*, *23*(12), Article 12. https://doi.org/10.1038/s41593-020-00744-x

Elliott, J. A., Mattingley, J. B., Eayrs, J. O., & Harris, A. M. (2025). *Individual differences in perceptual capacity depend on aperiodic slope, not alpha oscillations* (p. 2025.07.21.666053). bioRxiv. https://doi.org/10.1101/2025.07.21.666053

Foxe, J. J., & Snyder, A. C. (2011). The Role of Alpha-Band Brain Oscillations as a Sensory Suppression Mechanism during Selective Attention. *Frontiers in Psychology*, *2*, 154. https://doi.org/10.3389/fpsyg.2011.00154

Fries, P. (2005). A mechanism for cognitive dynamics: Neuronal communication through neuronal coherence. *Trends in Cognitive Sciences*, *9*(10), 474–480. https://doi.org/10.1016/j.tics.2005.08.011

Gallego-Rudolf, J., Wiesman, A. I., Pichet Binette, A., Villeneuve, S., & Baillet, S. (2024). Synergistic association of Aβ and tau pathology with cortical neurophysiology and cognitive decline in asymptomatic older adults. *Nature Neuroscience*, *27*(11), 2130–2137. https://doi.org/10.1038/s41593-024-01763-8

Gao, R., Peterson, E. J., & Voytek, B. (2017). Inferring synaptic excitation/inhibition balance from field potentials. *NeuroImage*, *158*, 70–78. https://doi.org/10.1016/j.neuroimage.2017.06.078

Groppe, D. M., Bickel, S., Keller, C. J., Jain, S. K., Hwang, S. T., Harden, C., & Mehta, A. D. (2013). Dominant frequencies of resting human brain activity as measured by the electrocorticogram. *NeuroImage*, *79*, 223–233. https://doi.org/10.1016/j.neuroimage.2013.04.044

Gross, J., Baillet, S., Barnes, G. R., Henson, R. N., Hillebrand, A., Jensen, O., Jerbi, K., Litvak, V., Maess, B., Oostenveld, R., Parkkonen, L., Taylor, J. R., van Wassenhove, V., Wibral, M., & Schoffelen, J.-M. (2013). Good practice for conducting and reporting MEG research. *NeuroImage*, *65*, 349–363. https://doi.org/10.1016/j.neuroimage.2012.10.001

Gyurkovics, M., Clements, G. M., Low, K. A., Fabiani, M., & Gratton, G. (2022). Stimulus-Induced Changes in 1/f-like Background Activity in EEG. *Journal of Neuroscience*, *42*(37), 7144–7151. https://doi.org/10.1523/JNEUROSCI.0414-22.2022

Heinrichs-Graham, E., Kurz, M. J., Becker, K. M., Santamaria, P. M., Gendelman, H. E., & Wilson, T. W. (2014). Hypersynchrony despite pathologically reduced beta oscillations in patients with Parkinson's disease: A pharmaco-magnetoencephalography study. *Journal of Neurophysiology*, *112*(7), 1739–1747. https://doi.org/10.1152/jn.00383.2014

Herrmann, C. S., Strüber, D., Helfrich, R. F., & Engel, A. K. (2016). EEG oscillations: From correlation to causality. *International Journal of Psychophysiology*, *103*, 12–21. https://doi.org/10.1016/j.ijpsycho.2015.02.003

Hill, A. T., Clark, G. M., Bigelow, F. J., Lum, J. A. G., & Enticott, P. G. (2022). Periodic and aperiodic neural activity displays age-dependent changes across early-to-middle childhood. *Developmental Cognitive Neuroscience*, *54*, 101076. https://doi.org/10.1016/j.dcn.2022.101076

Jensen, O. (2024). Distractor inhibition by alpha oscillations is controlled by an indirect mechanism governed by goal-relevant information. *Communications Psychology*, *2*(1), 1–11. https://doi.org/10.1038/s44271-024-00081-w

Jensen, O., & Mazaheri, A. (2010). Shaping Functional Architecture by Oscillatory Alpha Activity: Gating by Inhibition. *Frontiers in Human Neuroscience*, *4*, 186. https://doi.org/10.3389/fnhum.2010.00186

Koenig, L., & He, B. J. (2025). Spontaneous slow cortical potentials and brain oscillations independently influence conscious visual perception. *PLOS Biology*, *23*(1), e3002964. https://doi.org/10.1371/journal.pbio.3002964

Landry, M., da Silva Castanheira, J., Raz, A., Baillet, S., & Sackur, J. (2024). A lateralized alpha-band marker of the interference of exogenous attention over endogenous attention. *Cerebral Cortex*, *34*(1), bhad457. https://doi.org/10.1093/cercor/bhad457

Lendner, J. D., Helfrich, R. F., Mander, B. A., Romundstad, L., Lin, J. J., Walker, M. P., Larsson, P. G., & Knight, R. T. (2020). An electrophysiological marker of arousal level in humans. *eLife*, *9*, e55092. https://doi.org/10.7554/eLife.55092

Limbach, K., & Corballis, P. M. (2016). Prestimulus alpha power influences response criterion in a detection task. *Psychophysiology*, *53*(8), 1154–1164. https://doi.org/10.1111/psyp.12666

Lu, R., Dermody, N., Duncan, J., & Woolgar, A. (2024). Aperiodic and oscillatory systems underpinning human domain-general cognition. *Communications Biology*, *7*(1), 1–15. https://doi.org/10.1038/s42003-024-07397-7

Maschke, C., Duclos, C., Owen, A. M., Jerbi, K., & Blain-Moraes, S. (2023). Aperiodic brain activity and response to anesthesia vary in disorders of consciousness. *NeuroImage*, *275*, 120154. https://doi.org/10.1016/j.neuroimage.2023.120154

Medrano, J., Alexander, N. A., Seymour, R. A., & Zeidman, P. (2025). BSD: A Bayesian Framework for Parametric Models of Neural Spectra. *European Journal of Neuroscience*, *61*(10), e70149. https://doi.org/10.1111/ejn.70149

Merkin, A., Sghirripa, S., Graetz, L., Smith, A. E., Hordacre, B., Harris, R., Pitcher, J., Semmler, J., Rogasch, N. C., & Goldsworthy, M. (2022). Do age-related differences in aperiodic neural activity explain differences in resting EEG alpha? *Neurobiology of Aging*. https://doi.org/10.1016/j.neurobiolaging.2022.09.003

Merkin, A., Sghirripa, S., Graetz, L., Smith, A. E., Hordacre, B., Harris, R., Pitcher, J., Semmler, J., Rogasch, N. C., & Goldsworthy, M. (2023). Do age-related differences in aperiodic neural activity explain differences in resting EEG alpha? *Neurobiology of Aging*, *121*, 78–87. https://doi.org/10.1016/j.neurobiolaging.2022.09.003

Morrow, A., Elias, M., & Samaha, J. (2023). Evaluating the Evidence for the Functional Inhibition Account of Alpha-band Oscillations during Preparatory Attention. *Journal of Cognitive Neuroscience*, *35*(8), 1195–1211. https://doi.org/10.1162/jocn_a_02009

Mushtaq, F., Welke, D., Gallagher, A., Pavlov, Y. G., Kouara, L., Bosch-Bayard, J., van den Bosch, J. J. F., Arvaneh, M., Bland, A. R., Chaumon, M., Borck, C., He, X., Luck, S. J., Machizawa, M. G., Pernet, C., Puce, A., Segalowitz, S. J., Rogers, C., Awais, M., … Valdes-Sosa, P. (2024). One hundred years of EEG for brain and behaviour research. *Nature Human Behaviour*, *8*(8), 1437–1443. https://doi.org/10.1038/s41562-024-01941-5

Ostlund, B. D., Alperin, B. R., Drew, T., & Karalunas, S. L. (2021). Behavioral and cognitive correlates of the aperiodic (1/*f*-like) exponent of the EEG power spectrum in adolescents with and without ADHD. *Developmental Cognitive Neuroscience*, *48*, 100931. https://doi.org/10.1016/j.dcn.2021.100931

Ostlund, B., Donoghue, T., Anaya, B., Gunther, K. E., Karalunas, S. L., Voytek, B., & Pérez-Edgar, K. E. (2022). Spectral parameterization for studying neurodevelopment: How and why. *Developmental Cognitive Neuroscience*, *54*, 101073. https://doi.org/10.1016/j.dcn.2022.101073

Pilipenko, A., & Samaha, J. (2024). Double Dissociation of Spontaneous Alpha-Band Activity and Pupil-Linked Arousal on Additive and Multiplicative Perceptual Gain. *Journal of Neuroscience*, *44*(19). https://doi.org/10.1523/JNEUROSCI.1944-23.2024

R Core Team. (2022). *R: A Language and Environment for Statistical Computing*. R Foundation for Statistical Computing. https://www.R-project.org/

Rempe, M. P., Ott, L. R., Picci, G., Penhale, S. H., Christopher-Hayes, N. J., Lew, B. J., Petro, N. M., Embury, C. M., Schantell, M., Johnson, H. J., Okelberry, H. J., Losh, K. L., Willett, M. P., Losh, R. A., Wang, Y.-P., Calhoun, V. D., Stephen, J. M., Heinrichs-Graham, E., Kurz, M. J., & Wilson, T. W. (2023). Spontaneous cortical dynamics from the first years to the golden years. *Proceedings of the National Academy of Sciences*, *120*(4), e2212776120. https://doi.org/10.1073/pnas.2212776120

Romei, V., Brodbeck, V., Michel, C., Amedi, A., Pascual-Leone, A., & Thut, G. (2008). Spontaneous Fluctuations in Posterior α-Band EEG Activity Reflect Variability in Excitability of Human Visual Areas. *Cerebral Cortex*, *18*(9), 2010–2018. https://doi.org/10.1093/cercor/bhm229

Romei, V., Rihs, T., Brodbeck, V., & Thut, G. (2008). Resting electroencephalogram alpha-power over posterior sites indexes baseline visual cortex excitability. *NeuroReport*, *19*(2), 203. https://doi.org/10.1097/WNR.0b013e3282f454c4

Samaha, J., Bauer, P., Cimaroli, S., & Postle, B. R. (2015). Top-down control of the phase of alpha-band oscillations as a mechanism for temporal prediction. *Proceedings of the National Academy of Sciences*, *112*(27), 8439–8444. https://doi.org/10.1073/pnas.1503686112

Samaha, J., Iemi, L., Haegens, S., & Busch, N. A. (2020a). Spontaneous Brain Oscillations and Perceptual Decision-Making. *Trends in Cognitive Sciences*, *24*(8), 639–653. https://doi.org/10.1016/j.tics.2020.05.004

Samaha, J., Iemi, L., Haegens, S., & Busch, N. A. (2020b). Spontaneous Brain Oscillations and Perceptual Decision-Making. *Trends in Cognitive Sciences*, *24*(8), 639–653. https://doi.org/10.1016/j.tics.2020.05.004

Samaha, J., Iemi, L., & Postle, B. R. (2017). Prestimulus alpha-band power biases visual discrimination confidence, but not accuracy. *Consciousness and Cognition*, *54*, 47–55. https://doi.org/10.1016/j.concog.2017.02.005

Samaha, J., LaRocque, J. J., & Postle, B. R. (2022). Spontaneous alpha-band amplitude predicts subjective visibility but not discrimination accuracy during high-level perception. *Consciousness and Cognition*, *102*, 103337. https://doi.org/10.1016/j.concog.2022.103337

Samaha, J., & Postle, B. R. (2015). The Speed of Alpha-Band Oscillations Predicts the Temporal Resolution of Visual Perception. *Current Biology*, *25*(22), 2985–2990. https://doi.org/10.1016/j.cub.2015.10.007

Samaha, J., & Romei, V. (2024). Alpha-Band Frequency and Temporal Windows in Perception: A Review and Living Meta-analysis of 27 Experiments (and Counting). *Journal of Cognitive Neuroscience*, *36*(4), 640–654. https://doi.org/10.1162/jocn_a_02069

Schölvinck, M. L., Maier, A., Ye, F. Q., Duyn, J. H., & Leopold, D. A. (2010). Neural basis of global resting-state fMRI activity. *Proceedings of the National Academy of Sciences*, *107*(22), 10238–10243. https://doi.org/10.1073/pnas.0913110107

Singer, W. (2013). Cortical dynamics revisited. *Trends in Cognitive Sciences*, *17*(12), 616–626. https://doi.org/10.1016/j.tics.2013.09.006

Smit, C. M., Wright, M. J., Hansell, N. K., Geffen, G. M., & Martin, N. G. (2006). Genetic variation of individual alpha frequency (IAF) and alpha power in a large adolescent twin sample. *International Journal of Psychophysiology: Official Journal of the International Organization of Psychophysiology*, *61*(2), 235–243. https://doi.org/10.1016/j.ijpsycho.2005.10.004

Tadel, F., Baillet, S., Mosher, J. C., Pantazis, D., & Leahy, R. M. (2011). Brainstorm: A User-Friendly Application for MEG/EEG Analysis. *Computational Intelligence and Neuroscience*, *2011*, 1–13. https://doi.org/10.1155/2011/879716

Taylor, J. R., Williams, N., Cusack, R., Auer, T., Shafto, M. A., Dixon, M., Tyler, L. K., Cam-CAN, & Henson, R. N. (2017). The Cambridge Centre for Ageing and Neuroscience (Cam-CAN) data repository: Structural and functional MRI, MEG, and cognitive data from a cross-sectional adult lifespan sample. *NeuroImage*, *144*, 262–269. https://doi.org/10.1016/j.neuroimage.2015.09.018

Varela, F., Lachaux, J. P., Rodriguez, E., & Martinerie, J. (2001). The brainweb: Phase synchronization and large-scale integration. *Nature Reviews. Neuroscience*, *2*(4), 229–239. https://doi.org/10.1038/35067550

Voytek, B., Kramer, M. A., Case, J., Lepage, K. Q., Tempesta, Z. R., Knight, R. T., & Gazzaley, A. (2015). Age-Related Changes in 1/f Neural Electrophysiological Noise. *Journal of Neuroscience*, *35*(38), 13257–13265. https://doi.org/10.1523/JNEUROSCI.2332-14.2015

Wang, X.-J. (2010). Neurophysiological and Computational Principles of Cortical Rhythms in Cognition. *Physiological Reviews*, *90*(3), 1195–1268. https://doi.org/10.1152/physrev.00035.2008

Waschke, L., Donoghue, T., Fiedler, L., Smith, S., Garrett, D. D., Voytek, B., & Obleser, J. (2021). Modality-specific tracking of attention and sensory statistics in the human electrophysiological spectral exponent. *eLife*, *10*, e70068. https://doi.org/10.7554/eLife.70068

Weijs, M. L., Missura, S., Potok-Szybińska, W., Bächinger, M., Badii, B., Carro-Domínguez, M., Wenderoth, N., & Meissner, S. N. (2025). Modulating cortical excitability and cortical arousal by pupil self-regulation. *Nature Communications*, *16*(1), 4552. https://doi.org/10.1038/s41467-025-59837-5

Wen, H., & Liu, Z. (2016). Separating Fractal and Oscillatory Components in the Power Spectrum of Neurophysiological Signal. *Brain Topography*, *29*(1), 13–26. https://doi.org/10.1007/s10548-015-0448-0

Wiesman, A. I., Castanheira, J. da S., Degroot, C., Fon, E. A., Baillet, S., Group, P.-A. R., & Network, Q. P. (2022). *A sagittal gradient of pathological and compensatory effects of neurophysiological slowing in Parkinson's disease* (p. 2022.08.05.22278436). medRxiv. https://doi.org/10.1101/2022.08.05.22278436

Wiesman, A. I., da Silva Castanheira, J., & Baillet, S. (2022). Stability of spectral estimates in resting-state magnetoencephalography: Recommendations for minimal data duration with

neuroanatomical specificity. *NeuroImage*, *247*, 118823. https://doi.org/10.1016/j.neuroimage.2021.118823

Wiesman, A. I., da Silva Castanheira, J., Degroot, C., Fon, E. A., Baillet, S., & Network, Q. P. (2023). Adverse and compensatory neurophysiological slowing in Parkinson's disease. *Progress in Neurobiology*, *231*, 102538. https://doi.org/10.1016/j.pneurobio.2023.102538

Wiest, C., Torrecillos, F., Pogosyan, A., Bange, M., Muthuraman, M., Groppa, S., Hulse, N., Hasegawa, H., Ashkan, K., Baig, F., Morgante, F., Pereira, E. A., Mallet, N., Magill, P. J., Brown, P., Sharott, A., & Tan, H. (2023). The aperiodic exponent of subthalamic field potentials reflects excitation/inhibition balance in Parkinsonism. *eLife*, *12*, e82467. https://doi.org/10.7554/eLife.82467

Wilson, H. R., & Cowan, J. D. (1972). Excitatory and Inhibitory Interactions in Localized Populations of Model Neurons. *Biophysical Journal*, *12*(1), 1–24.

Wilson, L. E., Castanheira, J. da S., Kinder, B. L., & Baillet, S. (2024). Model selection for spectral parameterization. *bioRxiv*, 2024.08.01.606216. https://doi.org/10.1101/2024.08.01.606216

Wilson, L. E., da Silva Castanheira, J., & Baillet, S. (2022). Time-resolved parameterization of aperiodic and periodic brain activity. *eLife*, *11*, e77348. https://doi.org/10.7554/eLife.77348

Wöstmann, M., Waschke, L., & Obleser, J. (2019). Prestimulus neural alpha power predicts confidence in discriminating identical auditory stimuli. *European Journal of Neuroscience*, *49*(1), 94–105. https://doi.org/10.1111/ejn.14226

Xu, M., Han, B., Chen, Q., & Shen, L. (2025). Auditory stimuli extend the temporal window of visual integration by modulating alpha-band oscillations. *eLife*, *14*. https://doi.org/10.7554/eLife.105531.1

Zhou, Y. J., Iemi, L., Schoffelen, J.-M., Lange, F. P. de, & Haegens, S. (2021). Alpha Oscillations Shape Sensory Representation and Perceptual Sensitivity. *Journal of Neuroscience*, *41*(46), 9581–9592. https://doi.org/10.1523/JNEUROSCI.1114-21.2021

Supplemental Materials

	Log-detrended alpha power		
Predictors	*Estimates*	*CI*	*p*
(Intercept)	0.00	-0.02 – 0.02	1.000
Error in offset parameter	0.08	0.06 – 0.11	**<0.001**
Error in exponent parameter (1st order)	0.12	0.10 – 0.14	**<0.001**
Error in exponent parameter (2nd order)	0.61	0.59 – 0.63	**<0.001**
Observations	4935		
R^2 / R^2 adjusted	0.418 / 0.417		

Table S1. Error in estimating arrhythmic spectral parameters predicts log-detrended alpha power.

	Modelled alpha power		
Predictors	*Estimates*	*CI*	*p*
(Intercept)	-0.00	-0.03 – 0.02	0.796
Error in offset parameter	-0.09	-0.13 – -0.06	**<0.001**
Error in exponent parameter (1st order)	-0.04	-0.08 – -0.01	**0.006**
Error in exponent parameter (2nd order)	0.15	0.12 – 0.18	**<0.001**
Observations	4688		
R^2 / R^2 adjusted	0.031 / 0.030		

Table S2. Error in estimating arrhythmic spectral parameters weakly predicts modelled alpha power.

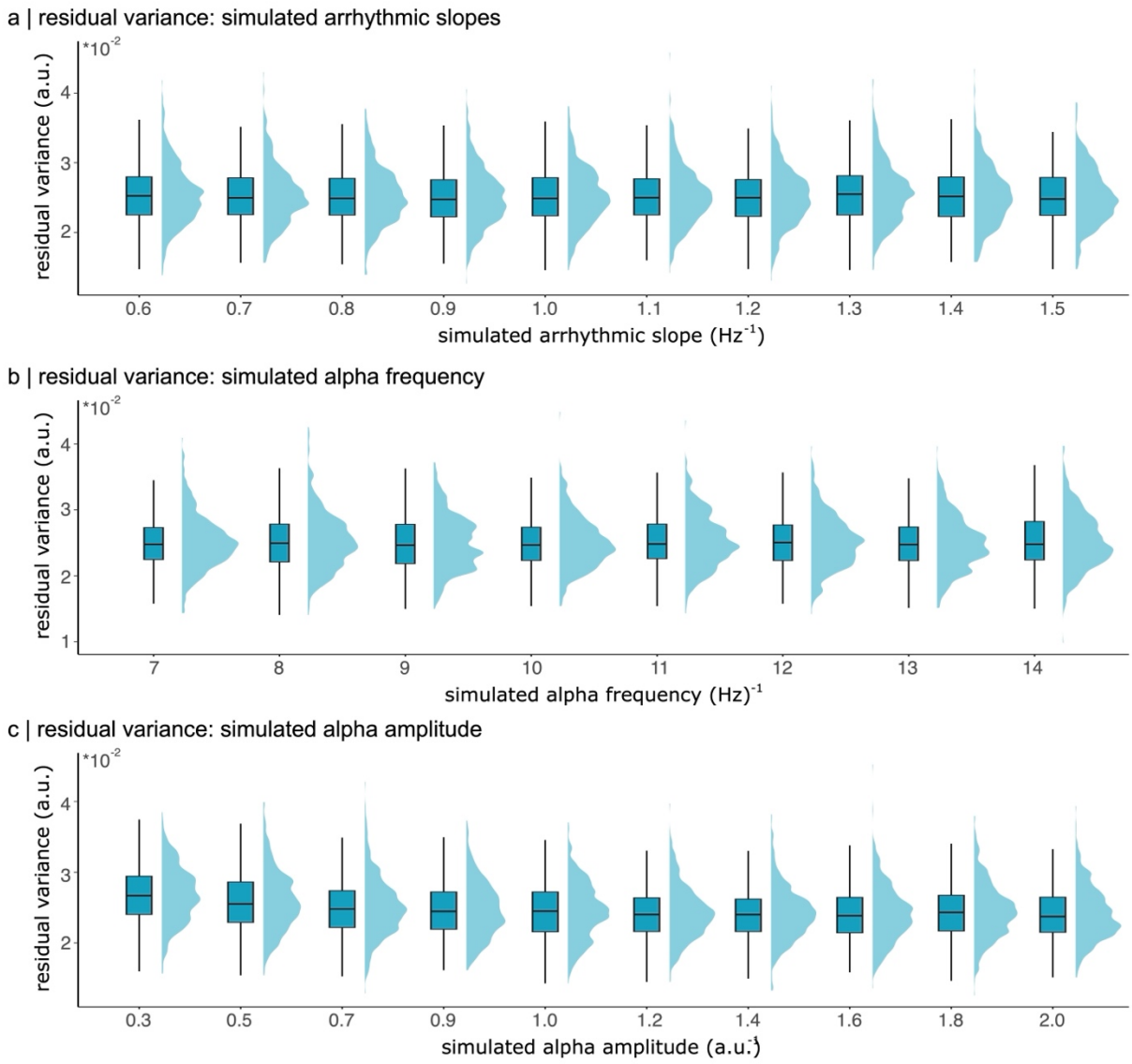

Figure S1. Residual variance of modelled spectra for all simulations.

Box plots of the residual model variance (i.e., mean squared error) for all simulations with no relationship between rhythmic alpha power and the arrhythmic exponent. We systematically simulated neural time series data to parameterize with varying levels of (a) arrhythmic exponent, (b) alpha centre frequencies, and (c) peak alpha amplitude. The model fit of *ms-specparam* did not systematically vary as a function of the simulated parameters.

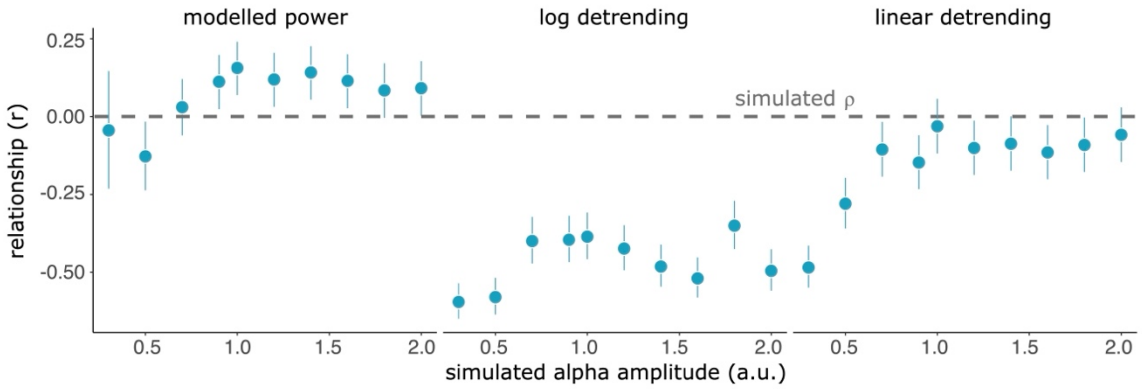

Figure S2. Spurious correlations between log detrended alpha power and exponent for different values of simulated amplitudes.

Scatter plot of the relationship between rhythmic alpha power and arrhythmic exponent for various values of simulated rhythmic alpha amplitude. Just as the results presented in the main text, modelled power computed as the maximum amplitude of modelled Gaussian peaks is the closest to the ground truth (i.e., $\rho = 0$, dashed grey line). In contrast, log- and linear- detrending of the power spectrum introduces systematic spurious correlations between estimated rhythmic alpha power and the arrhythmic exponent. This is most evident for the lowest amplitude peaks (peak amplitude < 0.7).

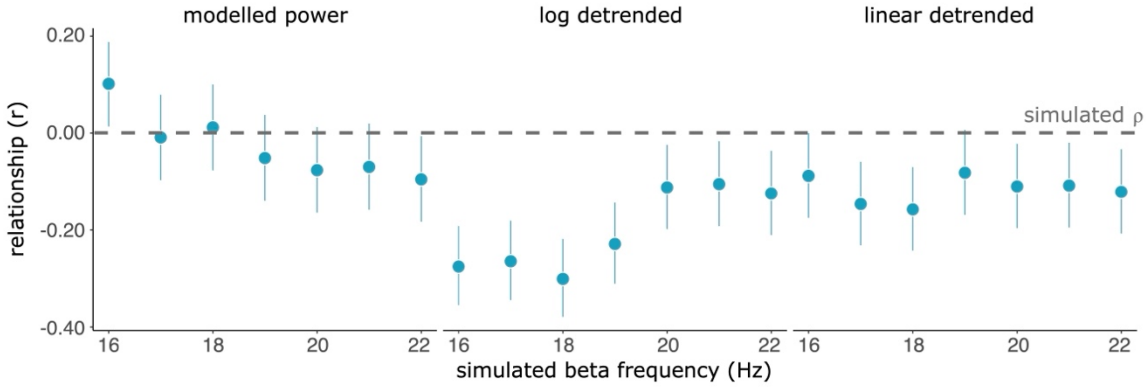

Figure S3. Spurious correlations between log detrended beta power and exponent.

To verify that the observed spurious relationships between rhythmic power and arrhythmic exponent are not specific to alpha rhythms, we simulated synthetic neural time series data and systematically varied beta peak centre frequency. Similar to the alpha peak centre frequency findings, modelled beta amplitudes were closer to the ground-truth relationship than log- and linear- detrended rhythmic beta power. Rhythmic beta power was weakly correlated to the arrhythmic exponent when computed using detrending methodology. This effect was most evident for low-beta (> 20 Hz).

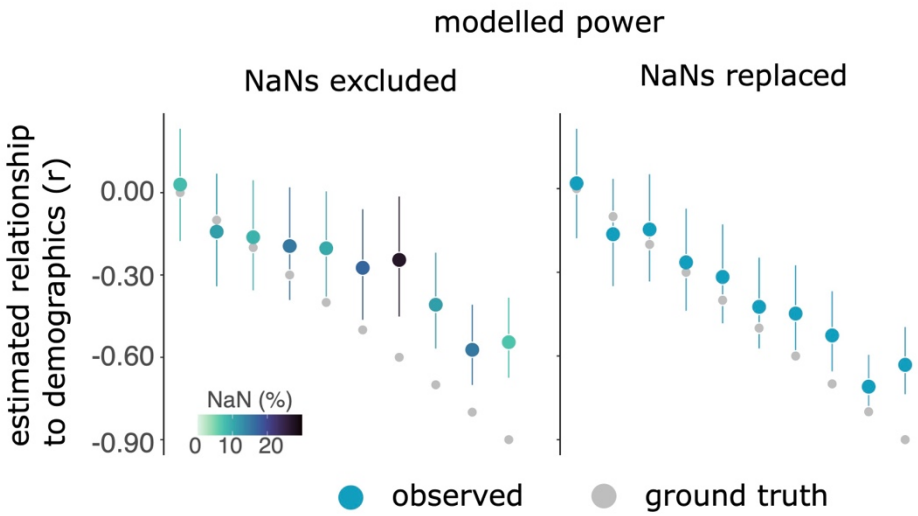

Figure S4. Modelled power recovers the relationship between alpha power and simulated demographic variables.

We simulated synthetic neural time series in which rhythmic alpha power was correlated to a simulated demographic variable. These analyses allowed us to determine how missing data—obtained when Gaussian peaks are not fit by *specparam*—impacts the relationship between observed behavioural/demographic variables and rhythmic power. Left panel: the estimated (coloured) vs ground truth simulated relationship between rhythmic alpha power and the simulated demographic variable. The colour of each point represents the proportion of missing amplitude values. We observed that Modelled power accurately recovered the simulated relationship when the effect size is small to medium ($\rho < 0.5$), but systematically underestimated the relationship for higher effect sizes ($\rho > 0.5$; left panel). In contrast, when replacing NaNs values of rhythmic power generated by *specparam* for 0, the estimated relationship is closer to the ground truth (right panel).

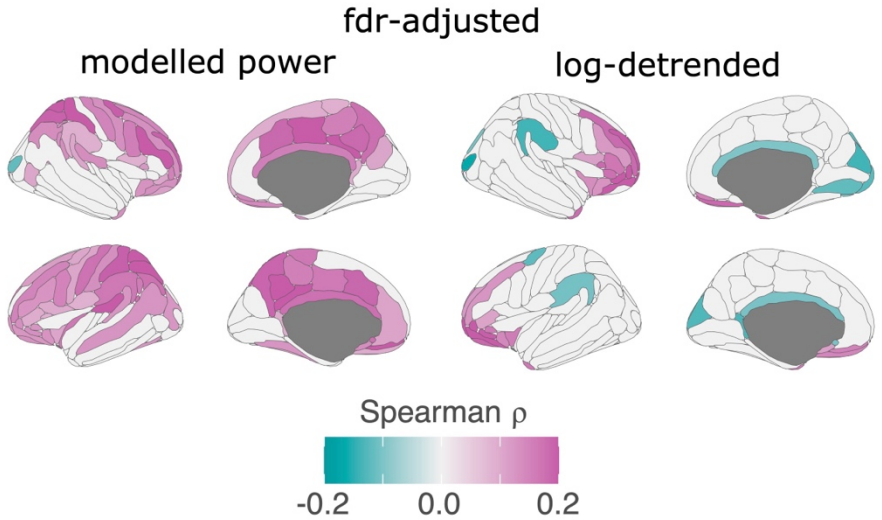

Figure S5. FDR-adjusted topographic map of the relationship between alpha power and exponent.

The relationship between arrhythmic exponent and rhythmic alpha power for each parcel of the Desterieux atlas modelled (left) and log-detrended power (right). The topographic maps are thresholded ($p_{FDR} < 0.05$) and depict significant relationships after correcting for multiple comparisons. While there are significant relationships between arrhythmic exponent and rhythmic alpha amplitude for both methods, the directionality and spatial extent of the relationship greatly depend on the method of quantifying rhythmic power.

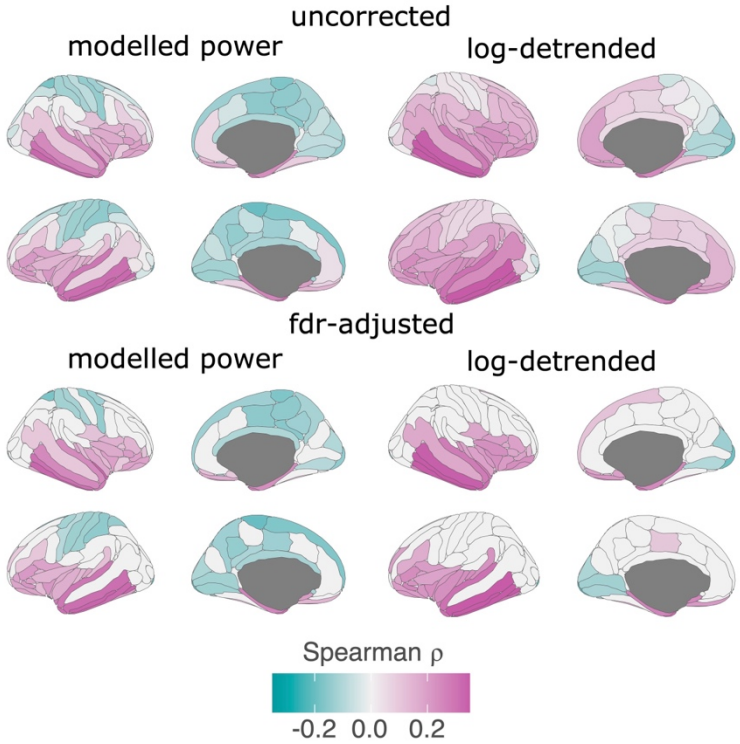

Figure S6. The relationship between resting-state alpha power and age diverges between modelling and detrending methods.

The relationship between rhythmic alpha power and chronological age for each parcel of the Desterieux atlas modelled (left) and log-detrended power (right). The unthresholded (top panel) and thresholded ($p_{FDR} < 0.05$, bottom panel) topographic maps demonstrate the differences in interpretation when utilizing different methods of quantifying rhythmic power. While age generally positively relates to log-detrended alpha power, this relationship inverts for modelled alpha power. We attribute these differences in findings to the arrhythmic exponent which is similarly altered by aging.

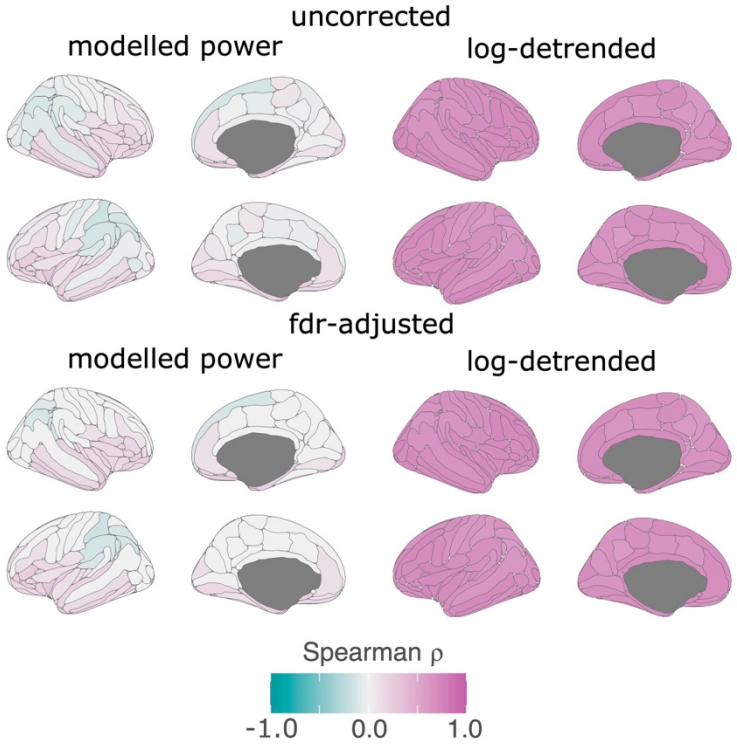

Figure S7. Topographic maps of the relationship between resting-state rhythmic alpha and beta power.

Topographic maps depicting the relationship between rhythmic alpha and beta power for each parcel of the Desterieux atlas based on modelled (left) and log-detrended power (right). The unthresholded (top panel) and thresholded ($p_{FDR} < 0.05$, bottom panel) topographic maps underscore the dramatic differences between both methodologies. Log-detrended power estimates (right panel) induce large correlations between the estimates of rhythmic alpha and beta power due to residual contributions of the arrhythmic exponent. In contrast, rhythmic alpha and beta power are weakly correlated to one another when relying on estimates of modelled power (left panel).

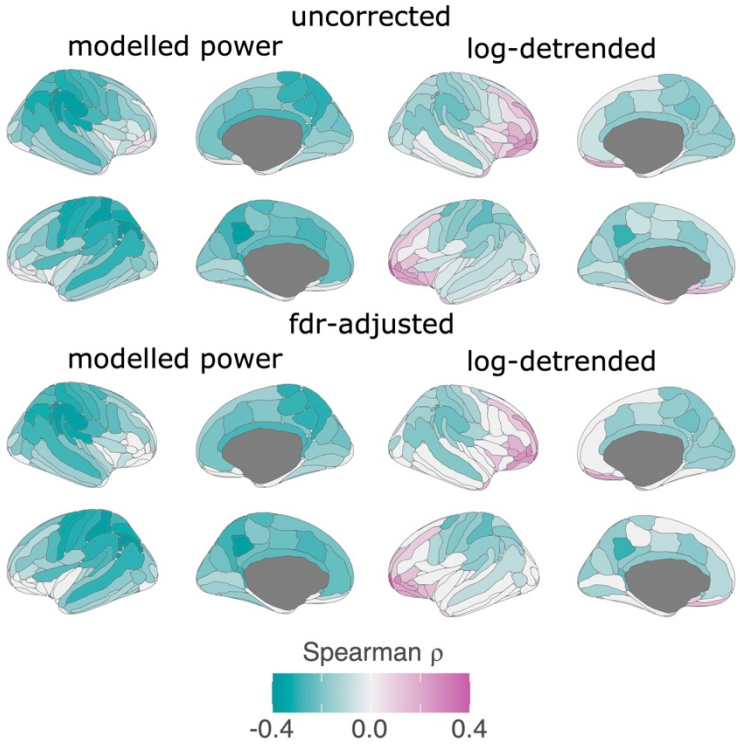

Figure S8. The relationship between resting-state beta power and arrhythmic exponent diverges between modelling and detrending methods.

The relationship between rhythmic beta power and arrhythmic exponent for each parcel of the Desterieux atlas modelled (left) and log-detrended power (right). The unthresholded (top panel) and thresholded ($p_{FDR} < 0.05$, bottom panel) topographic maps demonstrate the differences in interpretation when utilizing different methods of quantifying rhythmic power. While the arrhythmic exponent relates positively to frontal log-detrended beta power, this relationship inverts for modelled beta power.